

Universal Short-Distance Structure of the Single-Particle Spectral Function of Dilute Fermi Gases

William Schneider, Mohit Randeria

Department of Physics, The Ohio State University, Columbus, Ohio 43210

The universal $1/k^4$ tail in the momentum distribution of dilute Fermi gases implies that the spectral function $A(\mathbf{k}, \omega)$ must have weight below the chemical potential for large momentum $k \gg k_F$, with observable consequences in RF spectroscopy experiments. We show that this incoherent spectral weight is centered about $\omega \simeq -\epsilon(\mathbf{k})$ in a range of energies of order $v_F k$. This “bending back” in the dispersion, while natural for superfluids, is quite surprising for normal gases. We show that this universal structure is present in the hard-sphere gas as well as the Fermi liquid ground state of the highly imbalanced, attractive gas near unitarity. We argue that, even in the BCS superfluid, this bending back at large k is dominated by interaction effects which do not reflect the pairing gap.

PACS numbers: 03.75.Ss, 67.85.-d, 32.30.Bv

The spectral function $A(\mathbf{k}, \omega) = -\text{Im}G(\mathbf{k}, \omega + i0^+)/\pi$ of the single-particle Green’s function G is a quantity of fundamental interest in many-body physics [1, 2]. In addition to information about the spectrum and dynamics of single-particle excitations, it is also directly related to thermodynamic functions of an interacting many-particle system. Very recently there has been experimental progress in measuring (the occupied part of) $A(\mathbf{k}, \omega)$ in strongly interacting Fermi gases [3, 4], using a momentum-resolved version [5] of radio frequency (RF) spectroscopy [6, 7, 8]. These measurements [5] of $A(\mathbf{k}, \omega)$ for ultracold atomic gases are the analog of angle-resolved photoemission, which has given deep new insights into novel materials.

In this paper we uncover remarkable universal aspects of the short-distance structure of $A(\mathbf{k}, \omega)$ for dilute gases which leads to observable effects in RF experiments. Our investigation was motivated by the elucidation of the universal ultraviolet structure of various thermodynamic and equal-time correlations by Tan [9, 10]. One of his central results is the universal $k \gg k_F$ behavior of the momentum distribution $n_\sigma(\mathbf{k}) \simeq C/k^4$, where C is the “contact” [9, 10]. Using the $T = 0$ sum rule $\int_{-\infty}^0 d\omega A(\mathbf{k}, \omega) = n(\mathbf{k})$, this necessarily implies that $A(\mathbf{k}, \omega)$ has weight below the chemical potential ($\omega < 0$) for $k \gg k_F$. This is “incoherent” spectral weight, *not* associated with the coherent Landau quasiparticle.

We ask the question: Where is this incoherent spectral weight located for $k \gg k_F$? The surprising answer is that the incoherent part of the ω vs. k dispersion goes like $-\epsilon(\mathbf{k}) = -k^2/2m$, “bending back” away from the chemical potential at large k . While this is expected in BCS theory and its generalizations for a paired superfluid, we argue that this unusual dispersion is a universal feature of *all* dilute Fermi gases, even those with a *normal* (non-superfluid) ground state. We find that the spectral weight of C/k^4 in $A(\mathbf{k}, \omega)$ is centered about $\omega \simeq -\epsilon(\mathbf{k})$ in a range of energies of order $v_F k$ for normal Fermi gases. (Most of the spectral weight $(1 - C/k^4)$ is, of course, in the main branch of the dispersion centered about $\omega \approx +\epsilon(\mathbf{k})$, but these states are not occupied and

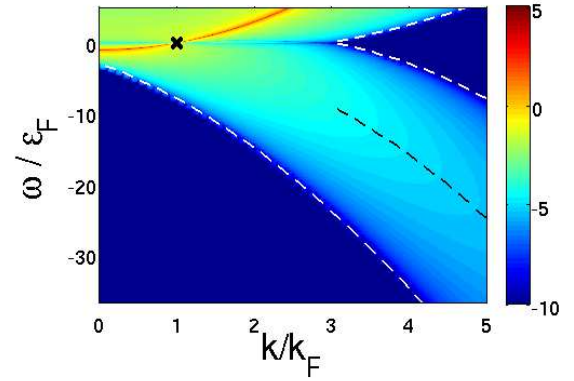


FIG. 1: (color online) Logarithmic intensity plot of $A(\mathbf{k}, \omega)$ for the repulsive Fermi gas ($k_F a = 0.1$; $na^3 = 3.4 \times 10^{-5}$). The red line is the quasiparticle. We focus here on the unusual dispersion centered about $\omega = -\epsilon(\mathbf{k})$ (black dashed line) in the range $\omega = -\epsilon(\mathbf{k}) - 3\epsilon_F \pm 2v_F k$ (white dashed lines) derived in the text.

do not contribute to the momentum distribution.)

We will first focus on two quite different situations where the ground state is a normal Fermi liquid: (a) the hard-sphere dilute Fermi gas, and (b) the highly imbalanced attractive Fermi gas, whose ground state is known to be normal. We will then turn to the case of a superfluid ground state, where we will argue that, in the BCS limit, the unusual dispersion is dominated by interaction effects rather than the effect of pairing. Finally we will conclude with implications for RF spectroscopy experiments.

Dilute repulsive Fermi gas: We begin with the simplest normal Fermi liquid in 3 dimensions, the hard sphere Fermi gas with dispersion $\epsilon(\mathbf{k}) = k^2/2m$, mass m , density $n = k_F^3/3\pi^2$, and scattering length $a > 0$ with $na^3 \ll 1$. (We will set $\hbar = k_B = 1$.) Its thermodynamic functions and Fermi liquid properties were studied in the classic papers of Galitskii and Lee, Yang and Huang; see Sec. 5 of [1]. The high- k tail was also calculated [11, 12]: $n(\mathbf{k}) \simeq (2/3\pi)^2 (k_F/k)^4$. Here we compute $A(\mathbf{k}, \omega)$.

In the low density limit $na^3 \ll 1$, the most important

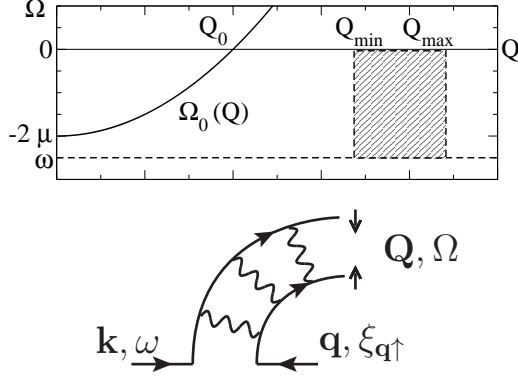


FIG. 2: (color online) Top: Kinematics of the processes that contribute to imaginary self-energy in eq. (1). $\text{Im}\Sigma$ is non-zero when the shaded rectangle (allowed by kinematics and thermal factors) overlaps with the region $\Omega > \Omega_0(Q)$ (in which $\text{Im}\Gamma$ is non-zero). This leads to the condition $Q_{\min} \leq Q_0$. Bottom: Diagram contributing to $\text{Im}\Sigma$.

physical process is repeated scattering in the particle-particle channel. The corresponding sum of ladder diagrams Γ is given by $\Gamma^{-1}(Q) = 1/g - L(Q)$, where $Q = (\mathbf{Q}, iQ_\ell)$ with $iQ_\ell = i2\ell\pi T$ and the bare interaction g is related to a via $1/g = m/(4\pi a) - \sum_{\mathbf{k}} 1/[2\epsilon(\mathbf{k})]$. Further $L(Q) = T \sum_k G^0(k+Q)G^0(-k)$ where $k = (\mathbf{k}, ik_n)$ with $ik_n = i(2n+1)\pi T$ and $G^0(k) = 1/[ik_n - \xi(\mathbf{k})]$ is the bare Green's function with the energy $\xi(\mathbf{k}) = \epsilon(\mathbf{k}) - \mu$ measured with respect to the chemical potential μ [13]. Note that one can obtain an analytically closed form expression [14] for $L(\mathbf{Q}, \Omega + i0^+)$. For the hard sphere gas we can make a further simplification $\Gamma \approx g + g^2 L$.

The Matsubara self-energy $\Sigma(k) = T \sum_q \Gamma(k+q)G^0(q)$ yields $\Sigma(\mathbf{k}, ik_n \rightarrow \omega + i0^+) = \text{Re}\Sigma + i\text{Im}\Sigma$, where

$$\text{Im}\Sigma(\mathbf{k}, \omega) = \sum_{\mathbf{q}} \text{Im}\Gamma(\mathbf{Q}, \Omega) [\Theta(-\xi(\mathbf{q})) - \Theta(-\Omega)] \quad (1)$$

at $T = 0$, with $\mathbf{Q} = \mathbf{k} + \mathbf{q}$ and $\Omega = \omega + \xi(\mathbf{q})$. $\text{Re}\Sigma$ is obtained by doing a Kramers-Kronig transform [15] on $\text{Im}\Sigma$. The integrations involved in Σ are performed numerically and the spectral function is obtained using $A(\mathbf{k}, \omega) = -\text{Im}[\omega - \xi(\mathbf{k}) - \Sigma(\mathbf{k}, \omega)]^{-1}/\pi$. We plot in Fig. 1, $A(\mathbf{k}, \omega)$ for the dilute, repulsive gas on a logarithmic intensity scale. We see the most intense feature, corresponding to the Landau quasiparticle near k_F , tracks $\omega \approx +\xi(\mathbf{k})$, up to many-body renormalizations [16]. However our main interest is in the much less intense, incoherent spectral feature that follows an $\omega = -\epsilon(\mathbf{k})$ dispersion and dominates $n(\mathbf{k})$ at large k .

To understand this “bending back” we write $A \approx |\text{Im}\Sigma(\mathbf{k}, \omega)|/[\pi(\omega - \epsilon(\mathbf{k}))^2]$ and we need to determine when $\text{Im}\Sigma(k, \omega)$ is non-zero for $k \gg k_F$ and $\omega < 0$. The simplest, qualitative answer comes from looking at the process shown in Fig. 2. We note that $\text{Im}\Gamma(\mathbf{Q}, \Omega) \neq 0$ only for small Q and Ω (as explained in detail below). Since $k \gg k_F$, we conclude that $\mathbf{q} \approx -\mathbf{k}$ so that

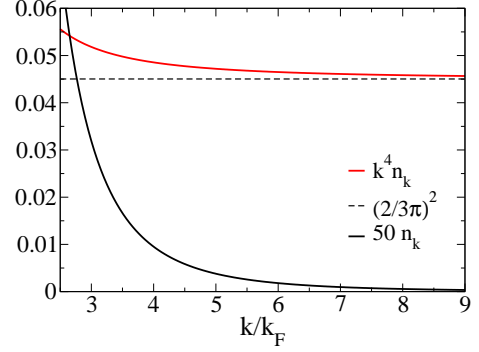


FIG. 3: (color online) Momentum distribution tail for the dilute repulsive Fermi gas with $na^3 = 3.4 \times 10^{-5}$.

$\mathbf{Q} = \mathbf{k} + \mathbf{q}$ is small with $Q \leq 2k_F$. We thus find $\xi(\mathbf{q}) \simeq \epsilon(\mathbf{k})$. The only way $\Omega = \omega + \xi(\mathbf{q})$ can be small is to demand $\omega \simeq -\epsilon(\mathbf{k})$.

To make this more quantitative we use eq. (1). From $\Omega = \xi(\mathbf{k} + \mathbf{Q}/2) + \xi(-\mathbf{k} + \mathbf{Q}/2)$ it follows that $\text{Im}\Gamma(\mathbf{Q}, \Omega) \neq 0$ when $\Omega \geq \Omega_0(Q) \equiv \epsilon(Q)/2 - 2\mu$; see Fig. 2. A second constraint $|\omega| \leq \Omega \leq 0$ follows from $\Omega = \xi(\mathbf{q}) + \omega$. The difference of Θ -functions in (1) implies $k_F \leq q \leq q_{\max} \equiv k_F [1 + |\omega|/\epsilon_F]^{1/2}$. Together with the kinematical constraint $|k - q| \leq Q \leq k + q$, this leads to $Q_{\min} = |k - q_{\max}|$. For non-zero $\text{Im}\Sigma$ we thus need the kinematically allowed region (shaded rectangle in Fig. 2) to overlap with $\Omega \geq \Omega_0(Q)$. This leads to the simple condition $Q_{\min} \leq Q_0$, where the definition $\Omega(Q_0) = 0$ leads to $Q_0 = 2k_F$. (We have also found, but do not discuss here, the $\omega > 0$ threshold for $A \neq 0$.)

Solving $|k - q_{\max}| = 2k_F$, we find that $A(\mathbf{k}, \omega < 0) \neq 0$ only in the range of energies described in the caption to Fig. 1. For $k \gg k_F$, this simplifies to $|\omega + \epsilon(\mathbf{k})| \leq 2v_F k$. Although the width of this energy range grows linearly with k , it becomes small relative to the central energy which grows like $-k^2$ for large k .

We plot in Fig. 3 the tail of the momentum distribution calculated using $\int_{-\infty}^0 d\omega A(\mathbf{k}, \omega)$ and find that it agrees with the analytical result [11]. This shows that the incoherent spectral weight in $A(k \gg k_F, \omega)$ contained in the interval $|\omega + \epsilon(\mathbf{k})| \leq 2v_F k$ is precisely C/k^4 .

Highly Imbalanced Attractive Fermi gas: We next turn to a single-channel attractive Fermi gas with two spin species whose scattering length a is tuned through a broad Feshbach resonance [17]. While the ground state for equal spin populations is known to be a superfluid exhibiting the BCS-BEC crossover, we consider the very different regime of large spin imbalance n_\uparrow/n_\downarrow . There is by now considerable body of theoretical work [18, 19] and experimental evidence [7, 8] that, for sufficiently large imbalance, superfluidity is destroyed for a large range of values of a , including unitarity $|a| = \infty$, and the ground state is a (partially polarized) normal Landau Fermi liquid.

At large scattering length we use the number of fermion species $2\mathcal{N}$ with an $Sp(2\mathcal{N})$ -invariant interaction as an

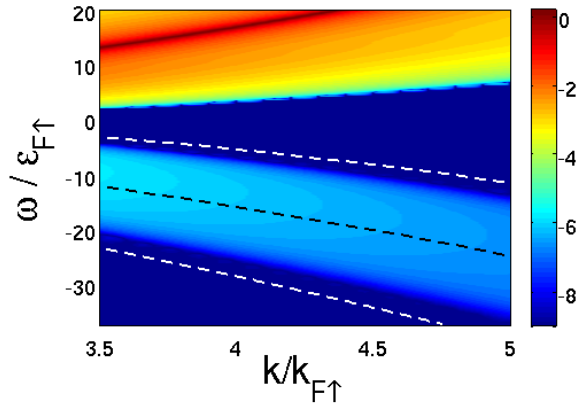


FIG. 4: (color online) Logarithm intensity plot of $A_k(\omega)$ for minority particles in the unitary Fermi gas with imbalance $n_{\downarrow}/n_{\uparrow} = 0.01$. The white dashed lines $\omega = -\epsilon(\mathbf{k}) \pm \alpha v_F k$ are derived in the text; the black dashed line is $\omega = -\epsilon(\mathbf{k})$.

artificial parameter to control the calculation in a large- \mathcal{N} expansion [14, 19]. To first order in $1/\mathcal{N}$, ladder diagrams in the p-p channel determine the self-energy. The resulting expressions are similar to those used above for the hard sphere gas, and we show them only schematically, highlighting the differences that arise from spin-imbalance, but omitting energy and momentum arguments. The only change in Γ is that $L = T \sum G_{\uparrow}^0 G_{\downarrow}^0$ where $G_{\sigma}^0(k) = 1/[ik_n - \xi_{\sigma}(\mathbf{k})]$ with $\xi_{\sigma}(\mathbf{k}) = \epsilon(\mathbf{k}) - \mu_{\sigma}$. The minority self-energy is then given by $\Sigma_{\downarrow} = T \sum \Gamma G_{\uparrow}^0$. $\text{Im}\Sigma_{\downarrow}$ is then given by eq. (1) with ξ replaced by ξ_{\uparrow} both in the Θ -function and in the definition of Ω .

We can analytically determine the range of energies within which $\text{Im}\Sigma$, and hence A , is non-zero using a very similar analysis to that for the hard sphere gas. In Fig. 2 we must now use $\Omega_0(Q) \equiv \epsilon(Q)/2 - 2\mu$ with $2\mu = \mu_{\uparrow} + \mu_{\downarrow}$. The final result is that, for $k \gg k_F$ and $\omega < 0$, $A(\mathbf{k}, \omega)$ can be non-zero only in the range of energies $|\omega + \epsilon(\mathbf{k})| \leq \alpha v_F k$ where $\alpha = \sqrt{2(1 + \epsilon_{F\downarrow}/\epsilon_{F\uparrow})}$. We have obtained more stringent bounds for the imbalanced case, using the detailed structure of $\text{Im}\Gamma$, but the simpler analysis described here suffices to establish a range linear in k centered about $-\epsilon(\mathbf{k})$.

For concreteness, we focus here on the unitary case ($|a| = \infty$). The result of our calculation of $A(\mathbf{k}, \omega)$ for the highly imbalanced ($n_{\downarrow}/n_{\uparrow} = 0.01$) unitary gas is shown in Fig. 4. Our calculation of $A(\mathbf{k}, \omega)$ is controlled only within the $1/\mathcal{N}$ -expansion. However, we note that the singularity structure in the large k limit is determined only by short-distance properties of the two-body problem in vacuum, while the strength of the singularity, namely C , depends on the many-body state. The ladder approximation (used in the $1/\mathcal{N}$ -expansion) is of course exact in so far as the two-body problem in vacuum is concerned. Thus we expect that the structure of the $k \gg k_F$, $\omega < 0$ spectral function, with its incoherent dispersion that bends back, to be robust beyond the $1/\mathcal{N}$ -expansion.

Superfluid State: We now turn to a discussion of the superfluid ground state for a system with *equal* densities of up and down spins and an interaction described by a scattering length a . Unlike the normal Fermi liquids described above, a branch of the dispersion that tracks $-\epsilon_{\mathbf{k}}$ at large k is very natural for the fermionic excitations in a superfluid [20]. Nevertheless, even in this case, our analysis gives important quantitative insights.

In BCS mean field theory the spectral function $A_{\text{MF}}(\mathbf{k}, \omega) = v_{\mathbf{k}}^2 \delta(\omega + E(\mathbf{k})) + u_{\mathbf{k}}^2 \delta(\omega - E(\mathbf{k}))$ where $v_{\mathbf{k}}^2 = 1 - u_{\mathbf{k}}^2 = [1 - \xi(\mathbf{k})/E(\mathbf{k})]/2$. The excitation energy $E(\mathbf{k}) = \sqrt{\xi^2(\mathbf{k}) + \Delta^2}$ with Δ the energy gap. For $k \gg k_F$, $E(\mathbf{k}) \approx \epsilon(\mathbf{k})$ and $v_{\mathbf{k}}^2 \approx \Delta^2/2\epsilon^2(\mathbf{k})$, so that $A_{\text{MF}}(k \gg k_F, \omega < 0) \approx [\Delta^2/2\epsilon^2(\mathbf{k})]\delta(\omega + \epsilon(\mathbf{k}))$. Thus we see that particle-hole mixing in the superfluid ground state naturally leads to a bending back of the dispersion.

However, there is a (large) quantitative problem with this result even in the BCS limit ($1/k_F a \ll -1$), where one might have expected it to be the most accurate. Using $n(\mathbf{k}) = \int_{-\infty}^0 d\omega A(\mathbf{k}, \omega)$, or directly from BCS theory, one finds that the momentum distribution $n_{\text{MF}}(\mathbf{k}) = v_{\mathbf{k}}^2 \approx \Delta^2/2\epsilon^2(\mathbf{k}) = C_{\text{MF}}/k^4$ for $k \gg k_F$. The problem is that the contact estimated from BCS theory $C_{\text{MF}} \sim \Delta^2 \sim \exp(-1/k_F |a|)$ is exponentially small in $|a|$. However, the exact answer [9, 10] in the BCS limit is $C = 4\pi^2 n^2 a^2$ as $a \rightarrow 0^-$. To understand why BCS theory gets the wrong answer for C we use the adiabatic relation [9] $d\mathcal{E}/da = \hbar^2 C/(4\pi m a^2)$. As shown in [21], interaction effects lead to power-law corrections in $|a|$ in the ground state energy density \mathcal{E} , which are numerically much more important than the essentially singular corrections coming from pairing. In the extreme BCS limit, the contact is dominated by the Hartree term in \mathcal{E} with calculable corrections [21].

Thus the actual $A(k \gg k_F, \omega < 0)$, even in the BCS limit, is dominated by interaction effects beyond BCS mean field theory. This results in a spectral weight $C \sim |a|^2$ arising from interaction effects which exist even in the normal state, rather than resulting from pairing, which only makes an exponentially small contribution.

Implications for RF spectroscopy: The physical effects we have discussed above lead to directly observable consequences in RF spectroscopy experiments where an RF pulse is used to transfer atoms from one hyperfine level to another. The interpretation of these experiments is often complicated by two difficulties: the inhomogeneity of trapped gases and severe final state interactions. The first problem has been solved in the usual (“angle-integrated”) RF experiments using tomographic techniques. Final state effects are not an issue in ^{40}K [5], and have been eliminated in ^6Li by suitable choice of hyperfine levels [7, 8]. We emphasize that but for this it would be very difficult to disentangle strong interactions in the many-body state (self energy effects) from final state effects (vertex corrections) [22]. We will thus work in the (now experimentally relevant) limit where we ignore all final state interactions.

Linear response theory then leads to the RF absorp-

tion intensity $I_\sigma(\mathbf{k}, \omega) = A_\sigma(\mathbf{k}, \xi_\sigma(\mathbf{k}) - \omega) f(\mathbf{k}, \xi_\sigma(\mathbf{k}) - \omega)$ where ω is the RF shift. The Fermi function $f(\omega)$ ensures that only occupied states can be excited by the probe. We set the multiplicative factor of the RF matrix element to unity so that $\int d\omega \sum_{\mathbf{k}} I_\sigma(\mathbf{k}, \omega) = N_\sigma$.

Angle-resolved RF experiments [5] directly probe (the occupied part of) the spectral function $A(\mathbf{k}, \omega)$ and thus its unusual dispersion for $k \gg k_F$, $\omega < 0$. The bending back is clearly visible in the published data [5] for attractive fermions near unitarity and near or above their critical temperature. But in this case it is hard to clearly separate the effects of the finite temperature pairing pseudogap [23] and normal state interaction effects. In particular, a bending back of the dispersion above T_c cannot by itself be used as evidence for a pairing pseudogap in view of the normal state results described here.

The consequences of our results for the angle-averaged RF experiments, which measure $I_\sigma(\omega) = \sum_{\mathbf{k}} I_\sigma(\mathbf{k}, \omega)$, are more subtle. We now show that unusual dispersion at large \mathbf{k} has a quantitative effect on the prefactor of the universal high- ω tail [24] in I_σ . We rewrite $I_\sigma(\omega) = \sum_{\mathbf{k}} \int_{-\infty}^0 d\Omega A_\sigma(\mathbf{k}, \Omega) \delta(\Omega - \xi_\sigma(\mathbf{k}) + \omega)$ at $T = 0$. In the $\omega \rightarrow \infty$ limit, large negative Ω values, centered

about $\Omega \approx -\epsilon(\mathbf{k})$, dominate. We thus find $I_\sigma(\omega \rightarrow \infty) \simeq \sum_{\mathbf{k}} n_\sigma(\mathbf{k}) \delta(\omega - 2\epsilon_{\mathbf{k}})$. Using [9] $n_\sigma(\mathbf{k}) \approx C/k^4$ for $k \gg k_F$ we thus find that $I_\sigma(\omega \rightarrow \infty) \approx (C/4\pi^2 \sqrt{m}) \omega^{-3/2}$. The characteristic power-law is independent of the phase (normal or superfluid) of the Fermi gas, though the value of C does depend on the many-body state.

Conclusions: We have shown that there is an unusual feature in the large momentum structure of the single-particle spectral function of *all* dilute Fermi gases, normal or superfluid, which is closely related to the universal short distance features discussed by Tan and others [9, 10]. This is an incoherent branch of the dispersion where ω goes like *negative* $\epsilon_{\mathbf{k}}$ [25] that is quite unexpected in a *normal* Fermi gas. Nevertheless, this is exactly what we find in the two systems where the ground state is known to be a normal Landau Fermi liquid: the hard sphere Fermi gas and the highly imbalanced, attractive Fermi gas. Even in a BCS superfluid, we show that this bending back at large k is dominated by interaction effects rather than the pairing gap.

Acknowledgments We acknowledge discussions with D. Jin and E. Taylor and support from nsf-dmr 0706203 and ARO W911NF-08-1-0338.

-
- [1] A. A. Abrikosov, L. P. Gorkov and I. Dzyaloshinski, *Methods of Quantum Field Theory in Statistical Physics*, (Dover, NY, 1963).
 - [2] L. Kadanoff and G. Baym, *Quantum Statistical Mechanics*, (Benjamin, 1962).
 - [3] I. Bloch, J. Dalibard and W. Zwerger, Rev. Mod. Phys. **80**, 885 (2008).
 - [4] S. Giorgini, L. P. Pitaevskii and S. Stringari, Rev. Mod. Phys. **80**, 1215 (2008).
 - [5] J. T. Stewart, J. P. Gaebler and D. S. Jin, Nature **454**, 744 (2008).
 - [6] C. Chin *et al.*, Science **305**, 1128 (2004).
 - [7] A. Schirotzek *et al.*, Phys. Rev. Lett. **101**, 140403 (2008).
 - [8] A. Schirotzek *et al.*, Phys. Rev. Lett. **102**, 230402 (2009).
 - [9] S. Tan, Ann. Phys. **323**, 2952 (2008); **323**, 2971 (2008) and **323**, 2987 (2008).
 - [10] E. Braaten and L. Platter, Phys. Rev. Lett. **100**, 205301 (2008); F. Werner, L. Tarruell and Y. Castin, Eur. Phys. J. B **68**, 401 (2009); S. Zhang and A. J. Leggett, Phys. Rev. A **79**, 023601 (2009).
 - [11] V. A. Belyakov, Sov. Phys. JETP **13**, 850 (1961). Note that [1] has a typographical error in its last equation of (5.24): the prefactor of k^{-4} is too large by a factor of 4.
 - [12] For a hard sphere gas $a = r_0$ the range of the potential (unlike $|a| \gg r_0$ in ref. [9]). Thus the “large” k regime here is $k_F \ll k \ll 1/a$.
 - [13] We use $\mu = \epsilon_F$ in L and G^0 since the corrections to μ are of order $k_F a$. This is also done for the large- N calculation for the polarized Fermi gas below.
 - [14] P. Nikolic and S. Sachdev, Phys. Rev. A **75**, 033608 (2007).
 - [15] The simplification $\Gamma \approx g + g^2 L$ for the hard sphere gas is valid only for $\omega \ll 1/ma^2$. $\text{Im}\Sigma$ grows indefinitely for larger ω . We subtract out this singular behavior $S(z) = -i(2\sqrt{2}/3\pi)(k_F a)^2 \sqrt{\epsilon_F z}$ and then Kramers-Kronig transform $\text{Im}\tilde{\Sigma} = \text{Im}\Sigma - \text{Im}S$. The real self-energy is then $\text{Re}\Sigma = \text{Re}\tilde{\Sigma} + \text{Re}S$.
 - [16] We have checked our numerics against known results [1] for chemical potential μ , quasiparticle residue Z , effective mass m^* , and the scattering rate near the Fermi surface.
 - [17] For the attractive Fermi gas $|a| \gg r_0$, the range, and we take $r_0 \rightarrow 0$.
 - [18] C. Lobo *et al.*, Phys. Rev. Lett. **97**, 200403 (2006); R. Combescot *et al.*, Phys. Rev. Lett. **98**, 180402 (2007); S. Pilati and S. Giorgini, Phys. Rev. Lett. **100**, 030401 (2008).
 - [19] M. Villetto *et al.*, Phys. Rev. A **78**, 033614 (2008); M. Veillette, D. Sheehy and L. Radzihovsky, Phys. Rev. A **75**, 043614 (2007).
 - [20] R. Haussmann, M. Punk, W. Zwerger; arXiv:cond-mat/0904.1333.
 - [21] R. B. Diener, R. Sensarma, and M. Randeria, Phys. Rev. A **77**, 023626 (2008); see Sec. VI and especially eq. (34).
 - [22] A. Perali, P. Pieri and G. Strinati, Phys. Rev. Lett. **100**, 010402 (2008).
 - [23] M. Randeria, in *Proc. Int. Sch. Phys. “Enrico Fermi” Course CXXXVI on High Temperature Superconductivity* ed. by G. Iadonisi, J. R. Schrieffer, and M. L. Chialfo, (IOS Press, 1998); cond-mat/9710223.
 - [24] Our result here corrects a factor of $\sqrt{2}$ in W. Schneider, V. Shenoy and M. Randeria; arXiv:cond-mat/0903.3006.
 - [25] After our work was complete we learned of R. Combescot, F. Alzetto and X. Leyronas, Phys. Rev. A **79**, 053640 (2009) where the approximation $\text{Im}\Sigma(k \gg k_F, \omega < 0) \propto \delta(\omega + \epsilon(\mathbf{k}))$ is used. While this may be sufficient for computing “integrated” quantities like $n(\mathbf{k})$, it does not capture the incoherent structure in $A(\mathbf{k}, \omega)$ described here.